Journal of Electronic Materials (2021) 50:5632–5638
https://doi.org/10.1007/s11664-021-09089-y

ORIGINAL RESEARCH ARTICLE

Characterization of Silver Nanoparticles Encapsulated Using an Ion-Exchange-Mediated Method and Their Application as Antimicrobial Agents

Y. Delgado-Beleño[1,2] · C. E. Martínez-Núñez[1,2] · N. S. Flores-López[3] · A. Meza-Villezcas[4] · L. P. Ramírez-Rodríguez[5] · R. Britto Hurtado[1] · M. Flores-Acosta[1] · M. Cortez-Valadez[6]

Received: 30 December 2020 / Accepted: 24 June 2021 / Published online: 10 July 2021

Abstract

This study presents a method to encapsulate silver nanoparticle clusters in a NaCl and zeolite 4A matrix. This process allowed clusters of silver nanoparticles (Ag NPs) smaller than 100 nm to be obtained, with a size trend of 7 nm. The interplanar distances obtained by transmission electron microscopy (TEM) support that the synthesized nanoparticles have a cubic structure. The optical properties of the encapsulated clusters were studied by considering the surface plasmon resonance of Ag NPs located around 374 nm. The antibacterial efficacy of encapsulated nanoparticles was analyzed based on minimum inhibitory concentration (MIC). The encapsulated Ag NPs showed antibacterial inhibition at relatively low doses.

Graphic Abstract

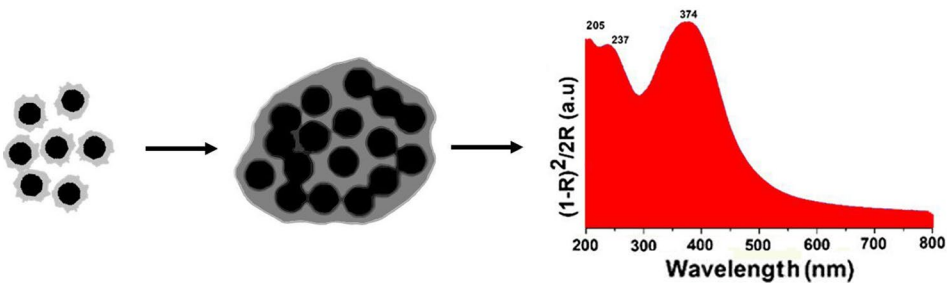

Keywords Silver encapsulated nanoparticles · optical properties · antimicrobial activity · confined clustering nanoparticles

Introduction

Nanostructured materials, particularly nanoparticles (NPs), are currently being highly studied due to their diverse properties, which are different in some applications than their bulk counterparts.[1–3] Nanoparticles find various uses due to their optical, thermal, electrical, magnetic, catalytic, and antimicrobial properties. Furthermore, nanoparticles have applications in medicine, biology, the energy industry, and pharmacology, among others.[4–7]

Recent studies have identified the following nanoparticles as antibacterial agents: Ag, Au, Cu, Zn, Ti, and silver oxide (Ag_2O), titanium dioxide (TiO_2), silicon (Si), copper oxide (II) (CuO), zinc oxide (ZnO), calcium oxide (II) (CaO), and magnesium oxide (MgO).[8,9] This feature has allowed the application of these agents in the treatment of infectious diseases, burns, food packaging and bottling, and coating of medical instruments.[10–12] The study of the antibacterial properties of nanoparticles has been increasing within the scientific community in recent years, as well as the synthesis of nanostructured materials. Studies of these antibacterial properties have been increasing, particularly due

✉ L. P. Ramírez-Rodríguez
patricio.ramirez@fisica.uson.mx

✉ R. Britto Hurtado
ricardoabritto@gmail.com

Extended author information available on the last page of the article

to the antibiotic resistance recently shown by many strains of bacteria.[13,14] Drug resistance is due to non-compliance with infection treatment, as well as the contamination of aquatic ecosystems caused by continuous contact with antimicrobial compounds from anthropogenic activities, such as waste from hospitals and urban wastewater, and their use in agriculture and aquaculture.[14,15] Antimicrobial resistance is reaching a critical point, where the efficiency of many of the main antimicrobial drugs is compromised. This issue represents a high risk for public health. Moreover, drug development programs will be unable to provide sufficient antimicrobial therapeutic coverage in the coming decades. An alternative solution to this issue is the implementation and use of nanoparticles with antimicrobial properties. Nanoparticles have a higher efficiency against pathogenic microorganisms due to their ultra-small size and a wide area/volume ratio.[16,17]

Moreover, recent results show advances in the functionalization of nanostructures with selected ligands and antibiotics. Better localization of bacteria and enhanced antimicrobial activity have also been achieved.[17,18] Also, the main advantages of these nanomaterials include solubility and minimal secondary effects. Additionally, nanomaterials exhibit multi-resistant microorganism targeting properties.[19,20]

Ag NPs show high antimicrobial activity and are currently considered a leading nanometric antimicrobial agent among the scientific community. Silver, in both ionic and metallic forms, shows high inhibition against a wide range of bacteria, including gram-negative and gram-positive bacteria. Such properties are shown even in small dosages.[21–24] The exact cytotoxicity mechanism of these materials is the focus of study, given that it depends on factors such as the bacteria and the size and material of the nanoparticle used. Literature shows that the main mechanisms of toxicity of the nanoparticles could be due to the generation of reactive oxygen species (ROS) or the progressive release of ions, which can damage or destroy the cell membrane. Finally, the adhesion of the nanoparticle to the cellular DNA, RNA, and protein molecules after penetrating the cytosol of the bacterium can lead to the disruption of different bacterial processes and subsequent cell death.[25,26]

On the other hand, obtaining nanoparticles immobilized in matrices has become a strength of materials science applications that require the stabilization of such nanomaterials for long periods.[27] Other authors have succeeded in stabilizing silver nanoparticles in polyethylene glycol (PEG), which improves the electrical conductivity of the compound.[28] Using short chains of carboxylic acid, Ankireddy et al. encapsulated silver nanoparticles for direct-write technology applications.[29] Teheri and co-workers succeeded in encapsulating silver nanoparticles in phospholipid bilayers by sonication for antibacterial applications.[30] Additionally, recent studies in this field have focused on sophisticated synthesis methods for stabilizing nanostructures, for example using polymer matrices, organic films, and membranes, among others.[31–34] These processes involve high costs, and biocompatibility is compromised in several cases. Therefore, synthesizing nanoparticles with antimicrobial properties in non-toxic matrices at a relatively low cost is an attractive method to obtain biocompatible materials for application in fields such as food packaging, textiles, medical device coating and treatment of infectious diseases.

This study addresses an attractive synthesis method for encapsulation and confinement of silver nanoparticles in a NaCl and Zeolite 4A matrix. A study of the bactericidal properties and inhibition parameters was carried out after the encapsulation of the nanoparticles.

Materials and Methods

Synthesis and Characterization

The nanoparticles were obtained in the NaCl matrix through the chemical reduction method. The synthesis process was carried out in three simple steps. The first step involves obtaining the zeolite 4A with Ag ions (samples: $4A+Ag^{+}$). In the second step, the metallic ions were incorporated in NaCl (solution $NaCl+Ag^{+}$). Lastly, in the third step, the ions in NaCl were reduced to obtain the encapsulated Ag NPs. Synthetic zeolite 4A obtained from Commercial Waco Chemicals, Inc. with a molecular formula $Na_{12}[(SiO_2)_{12}(AlO_2)_{12}]\ 27H_2O$ and sodium chloride (Fermont) were used as the matrices in the synthesis process. Silver nitrate ($AgNO_3$) (Fermont) was used as the precursor for the metallic ions. Polyethylenimine (PEI) and hydroxymethanesulfonate (Rongalite; $Na^{+}\ HOCH_2SO_2^{-}$) were the chemical reagents used as complexing and reducing agents, respectively. For a more detailed description of the synthesis process, see the supplementary data file.

In the characterization of the samples, the UV-Vis absorption spectra were obtained with a UV/Vis/near-IR PerkinElmer Lambda 19 spectrophotometer. The reflectance measurements were converted to absorbance data using Kubelka-Munk model. The morphology of the structure and the chemical composition of the nanoparticles were measured with the transmission electron microscopy (TEM; JEOL JEM-2010F, acceleration voltage, 200 KeV) coupled with an energy dispersive x-ray analysis (EDX) spectrometer. X-ray photoelectron spectroscopy (XPS) was used to obtain the electronic states of Ag atoms. These measurements were carried out in a SPECS spectrophotometer equipped with a PHOIBOS wide-angle lens electron energy analyzer using Al Kα (1486.6 eV, 200 W) as the excitation source. The obtained spectra were calibrated against

the C 1s peak at 285 eV. A global chemical analysis was carried out with inductively coupled plasma atomic emission spectroscopy (ICP-AES) using a Varian Liberty 110 spectrophotometer.

Antimicrobial Testing

Escherichia coli (clinically isolated) and *Staphylococcus aureus* (MC4100) bacterial strains were used for the analysis of the antibacterial response of encapsulated nanomaterials. An inoculum of both bacteria was incubated for ~16 h at 37°C in Luria-Bertani (LB) broth previously prepared with 1% tryptone, 1% sodium chloride, and 0.5% yeast extract, adjusting the PH to 7.5. Afterwards, dilutions were performed in series to obtain 1×10^4 cells per milliliter (cells/mL). All the culture media used were obtained with water distilled and sterilized by conventional methods.

The inhibitory response of the synthesized materials was evaluated by determining the minimum inhibitory concentration (MIC) following the well microdilution test. For this, 100 µl of the previously prepared inoculum was added to solutions of the ions and nanoparticles synthesized at concentrations of 2.0 µg/ml, 1.5 µg/ml, 1.0 µg/ml, and 0.5 µg/ml for both Ag^+ and Ag NPs. Afterwards, these cultures were incubated at 37°C from 18 to 24 h at 180 rpm. The solutions were prepared in LB broth, sterilized, and all the tests were done three times. The experiments were carried out in a 96-well U-bottom plate. After incubation, the treated cells were inoculated in a petri dish with agar LB (LB prepared as mentioned above with agar at 1.5%). To determine the MIC, the optical density of the bacteria treated with nanomaterials was measured at 600 nm in a Thermo Multiskan GO plate reader. Before the optical density measurement process, the treated cells were inoculated in a Petri dish with LB (LB prepared as mentioned above) agar (at 1.5%). Subsequently, the cells were re-incubated for ~16 h at 37°C to visualize the results.

Results and Discussion

The optical response of the encapsulated nanoparticles was studied with a diffuse reflectance spectroscope using the Kubelka-Munk model. Figure 1 shows the optical absorption spectra of encapsulated ions and Ag NPs in a NaCl and zeolite 4A matrix. The sample NaCl+Ag^+ shows three bands at 206 nm, 216 nm and 234 nm. The bands located at low wavelengths are associated with electronic transitions of Ag^+.[35] The encapsulated Ag NPs show two small bands at 205 nm and 237 nm, as well as a wide band, centered at 374 nm with a full width at half maximum (FWHM) of 84 nm. The bands localized at 205 nm and 237 nm are associated to the absorption of silver ions that remained in

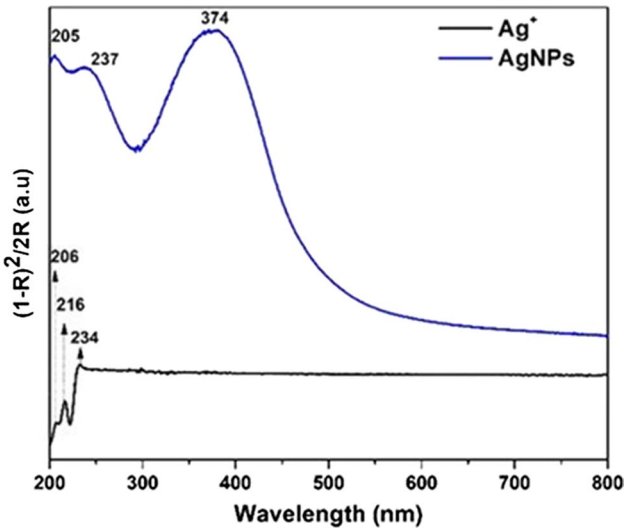

Fig. 1 Optical absorption spectra of both encapsulated Ag^+ and Ag NPs.

Table I Chemical compositions by ICP-AES of the ions and Ag NPs stabilized in NaCl.

Atomic (%)	
NaCl+Ag^+	NaCl+AgNPs
1.0	1.0

the sample after the reduction process. On the other hand, the wide band centered at 374 nm is a result of the surface plasmon resonance (SPR) of approximately 7 nm spherical silver nanoparticles, which is later confirmed by TEM. The wide FWHM of the band located at 374 nm can be ascribed to the SPR coupling of Ag NPs of different sizes that were left close to the others. This proximity is due to relatively small dispersion of the nanoparticles. On the other hand, the imperfect spherical shape of the nanoparticles can also produce a higher order resonance than the typical dipolar resonance of spherical nanoparticles. Such resonances are found at slightly higher wavelengths than the dipolar that could overlap and allow a wider FWHM for these nanoparticles.[36]

The global chemical composition of the encapsulated nanoparticles was analyzed by ICP-AES; the results are shown in Table I. The table shows that the materials with Ag have a high atomic percentage. This is possibly because zeolites have a higher affinity of ion exchange with silver ions than other metal ions.[37] NaCl can be soluble in water, and in the absence of water, crystals form again. We assume that both ions and nanoparticles interstitially interact with the crystal lattice of NaCl. The synthesis process described herein takes advantage of this condition in combination with the zeolite to encapsulate the nanoparticles, providing higher stability.

Morphology, structure, and elemental composition (almost punctual) of the samples were studied in TEM and

EDS. Figure 2a and b shows encapsulated and confined silver particles around 100 nm in diameter. Figure 2c shows a micrograph of Ag NPs distributed in NaCl. These figures allow us to identify a crystal plane with an interplanar distance of 2.34 Å. This distance corresponds to a plane with Miller indices (111) of the cubic structure of silver (PDF

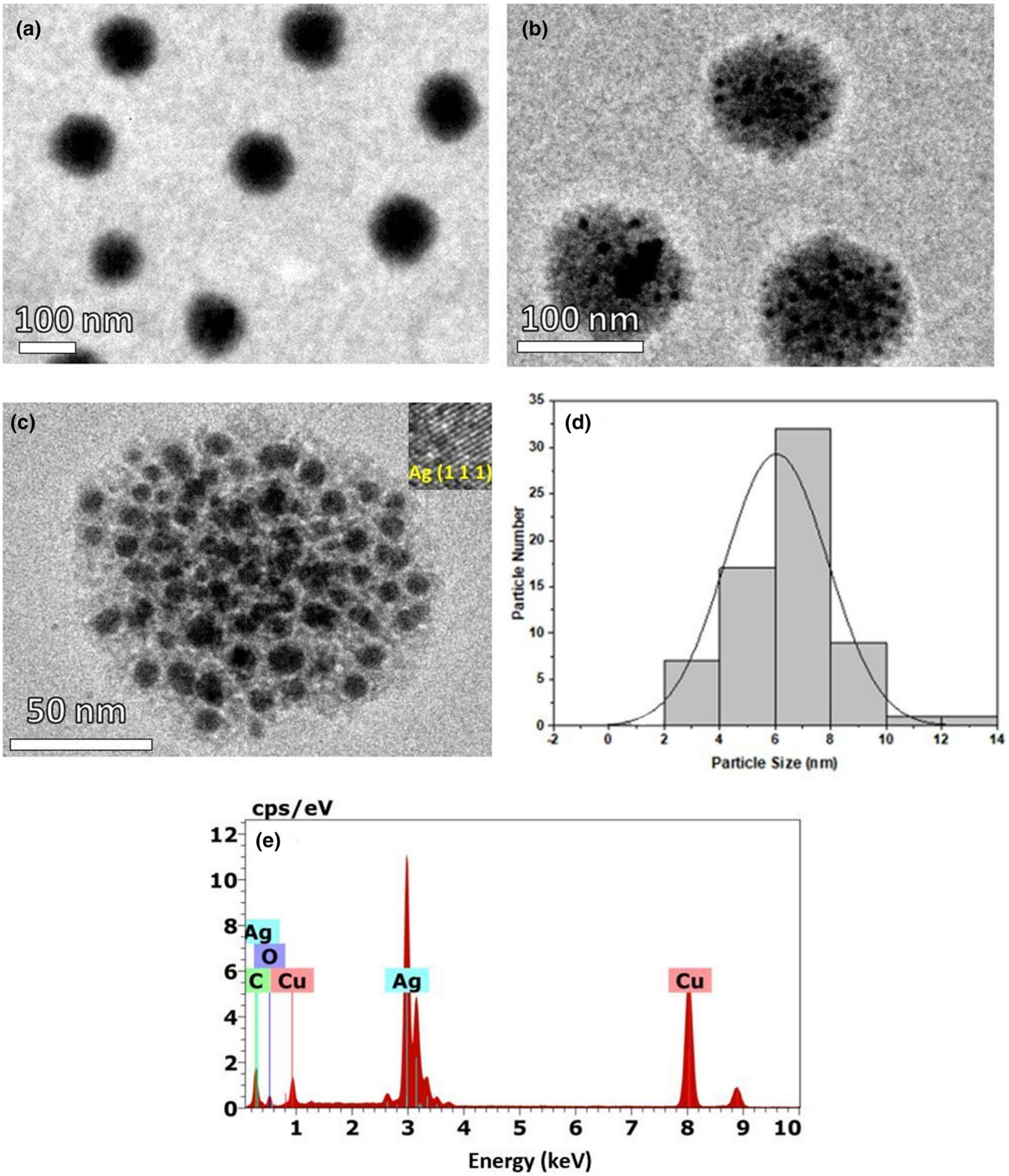

Fig. 2 TEM images of: (a–c) encapsulated Ag NPs, (d) particle size histogram of (c), and (e) EDS spectrum.

code: 4-0783). This micrograph shows that most of the nanoparticles have a spherical morphology located inside a cloud of NaCl. It is also possible to observe that the distribution of the size of the nanoparticles is quite uniform. The particle size of the micrography shown in Fig. 2c allowed us to obtain a distribution of the synthesized nanoparticles. The histogram shows that most nanoparticles have a size between 4 nm and 8 nm, with a predominant size of 7 nm (Fig. 2d). Figure 2e displays almost punctual spectra of EDS taken from an isolated nanoparticle, which shows the different elements that constitute the sample. Transition energies of L_α = 2.983 KeV typical of electronic transitions of silver are shown.[38] Cu shown in this spectrum belongs to the grid used for the measurement of the sample. These results show that the synthesis method used can produce Ag nanoparticles with good uniformity and a size of a few nanometers.

The oxidation state of the synthesized nanostructures was studied by XPS. Figure 3 shows the images of the low-resolution spectra and the high-resolution spectra of the encapsulated Ag NPs. Figure 4a shows the spectra of NaCl. These spectra show binding energy of different orbitals of the elements in the sample, such as Cl, Na, O and N (belongs to PEI), as well as Ag. After fitting and deconvolution to the carbon peak at 285 eV in the high-resolution spectrum (shown in Fig. 4b), two signals of $Ag3d_{3/2}$ and $Ag3d_{5/2}$ were visible with associated binding energies at 374.2 and 368.2 eV, respectively. These signals correspond to the existing doublet for Ag atoms. The signal observed at 368.2 eV and the difference of 6 eV in the binding energies with the peak at 374.2 eV is associated with Ag^0.[39] It is known that these binding energies can show small shifts that depend on the synthesis medium of the nanoparticles.[40] For Ag NPs with sizes smaller than 10 nm, the binding energies of the Ag 3d orbitals show slight shifts to higher binding energies. This

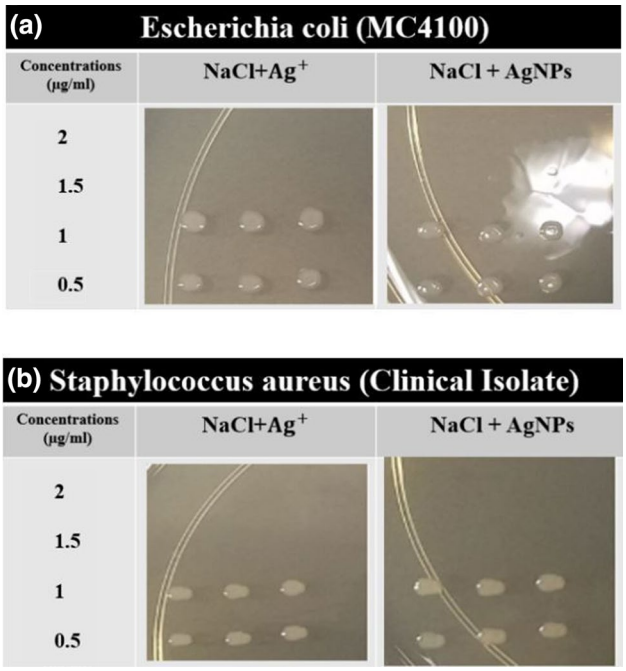

Fig. 4 Images of stamping on the petri dishes after the incubation of the samples NaCl+Ag^+ and NaCl+AgNPs at different concentrations over the bacteria: (a) *E. coli* and (b) *S. aureus*.

shows that our results agree with the results reported in the literature.

The antibacterial response of the synthesized encapsulated nanoparticles was analyzed by determining the MIC of the materials against *E. coli* and *S. aureus*. Figure 4 shows the images of the stamping done on the petri dish of the *E. coli* strain as well as for the *S. Aureus* strain with four different concentrations of the synthesized nanomaterials. The concentrations tested were 2 µg/mL, 1.5

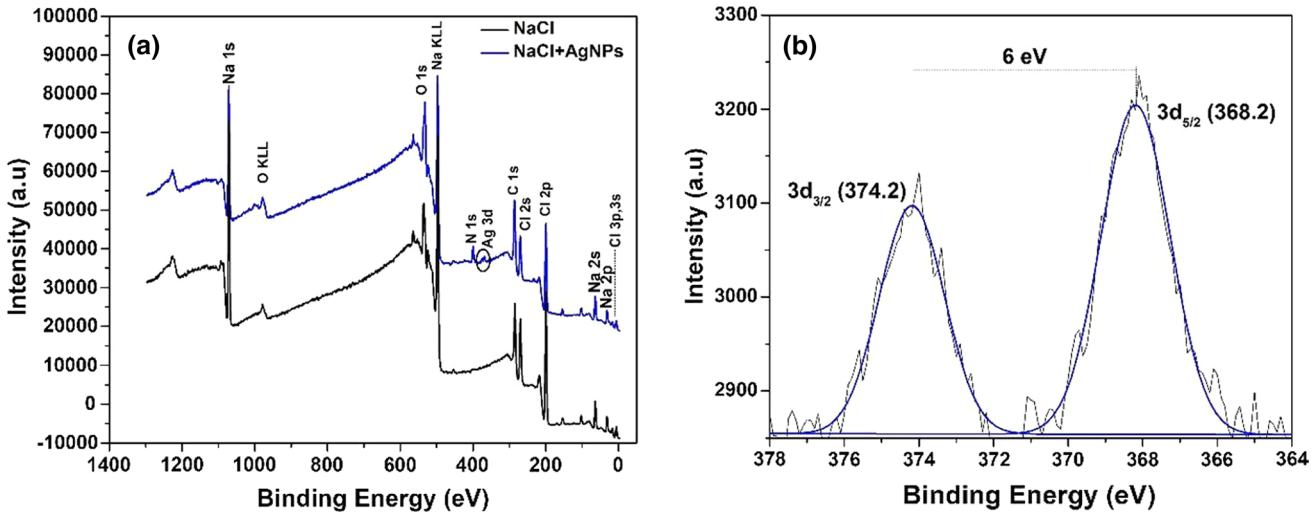

Fig. 3 (a) Low-resolution XPS of NaCl and sample NaCl+AgNPs and (b) high-resolution XPS of Ag 3d orbitals in NaCl.

μg/mL, 1 μg/mL, 0.5 μg/mL for the samples containing silver. The images show no growth in the inocula treated with concentrations of 2 and 1.5 μg/mL silver contained in the samples NaCl+Ag^+ and encapsulated Ag NPs for both bacteria. Table II shows the MIC of the different materials synthesized towards both bacteria. This table shows that the MIC of Ag^+ and encapsulated Ag NPs with both bacteria are relatively low, even when compared with the results obtained in other studies.[41] Values of 1.5 μg/mL were obtained for encapsulated Ag NPs and Ag^+ on the bacteria *E. coli.* It is known that silver, in ionic and nanoparticle form, shows an excellent inhibitory response against a wide range of bacteria.[42,43] However, these results indicate that the antibacterial activity, when tested in NaCl, is higher than previously reported for this material in an aqueous solution.[41]

The action mechanism of the nanoparticles on the bacteria needs to be further studied. However, several studies suggest three main action modes through which silver nanoparticles can inhibit antibacterial growth. The first one is occupied by the progressive release of ions from the nanoparticle, which leads to the exhaustion of the antioxidant capacity and inactivation of the metabolic functions of the bacteria. Secondly, the generation of reactive oxygen species (ROS) can damage the microbial DNA, proteins, and the cell membrane.[26] Finally, the penetration of nanoparticles in the cell wall and adhering to the cell membrane can prevent metabolic processes in the bacteria and cause structural changes, which would eventually lead to its death.[44] It is possible to suppose that the cytotoxicity of nanoparticles against *E. coli* and *S. aureus* bacteria is due to the progressive release of ions from the nanoparticle, which tend to accumulate in the bacterial membrane and then enter the cytosol to bind to enzymes and proteins, thereby causing cell death. We assume that the enhanced bactericidal effect of small particles occurs since the amount of ions released per unit mass is higher in small particles. The encapsulated silver nanoparticles obtained in this work can become attractive for drug delivery applications, as they have a relatively low production cost. However, it is necessary to conduct such studies in the future to corroborate their successful performance.

Table II MIC of the samples NaCl+Ag^+ and NaCl+AgNPs, as well as controls (NaCl), over the bacteria *E. coli* and *S. aureus*.

Samples	MIC (μg/ml)	
	S. aureus	*E. coli*
NaCl+Ag^+	1.5	2
NaCl+AgNPs	1.5	2
NaCl	45	45

Conclusions

The use of NaCl and zeolite 4A matrix in the synthesis of nanoparticles provides a straightforward and economical route to obtain encapsulated Ag NPs with a quasi-uniform distribution and size below 7 nm. According to TEM, the nanostructures obtained have a spherical morphology, and the measured interplanar distances predict a cubic structure. The optical response of the nanoparticles shows surface plasmon resonances at 374 nm for encapsulated Ag NPs, which confirms the stabilization of the nanoparticles in NaCl. This method also allows the synthesis of nanoparticles with possibly low toxicity due to the reactants used in the process.

The antibacterial activity evaluated against *E. coli* MC4100 and clinically isolated *S. aureus* bacteria shows that the encapsulated Ag NPs have excellent bactericidal activity. These results confirm that encapsulated and confined Ag NPs are excellent prospects for potential use as antibacterial agents.

Supplementary Information The online version contains supplementary material available at https://doi.org/10.1007/s11664-021-09089-y.

Acknowledgments This work was supported by the A1-S-46242 Project of the CONACYT Basic Science. The author M. Cortez-Valadez appreciates support from the "Cátedras CONACYT" program. Special thanks are also extended for the support by the Laboratory of Transmission Electron Microscopy at the University of Sonora. R. Britto Hurtado acknowledges to Postdoctoral Fellowship by CONACYT Mexico.

Conflict of interest The authors declare that they have no conflict of interest.

References

1. G. Bodelón, C. Costas, J. Pérez-Juste, I. Pastoriza-Santos, and L.M. Liz-Marzán, *Nano Today* 13, 40 (2017).
2. M. Baghayeri, A. Amiri, and S. Farhadi, *Sens. Actuators B Chem.* 225, 354 (2016).
3. G. Zheng, L. Polavarapu, L.M. Liz-Marzán, I. Pastoriza-Santos, and J. Pérez Juste, *Chem. Commun.* 51, 4572 (2015).
4. A. Kaler, A.K. Mittal, M. Katariya, H. Harde, A.K. Agrawal, S. Jain, and U.C. Banerjee, *J. Nanopart. Res.* 16, 2605 (2014).
5. M. Kapilashrami, Y. Zhang, Y.-S. Liu, A. Hagfeldt, and J. Guo, *Chem. Rev.* 114, 9662 (2014).
6. A. Zaleska-Medynska, M. Marchelek, M. Diak, and E. Grabowska, *Adv. Colloid Interface Sci.* 229, 80 (2016).
7. R. Sridhar, R. Lakshminarayanan, K. Madhaiyan, V.A. Barathi, K.H.C. Lim, and S. Ramakrishna, *Chem. Soc. Rev.* 44, 790 (2015).
8. S.M. Dizaj, F. Lotfipour, M. Barzegar-Jalali, M.H. Zarrintan, and K. Adibkia, *Mater. Sci. Eng. C* 44, 278 (2014).
9. T. Gordon, B. Perlstein, O. Houbara, I. Felner, E. Banin, and S. Margel, *Colloids Surf. A* 374, 1 (2011).
10. H. Zazo, C.I. Colino, and J.M. Lanao, *J. Control. Release* 224, 86 (2016).
11. F. Oyarzun-Ampuero, A. Vidal, M. Concha, J. Morales, S. Orellana, and I. Moreno-Villoslada, *Curr. Pharm. Des.* 21, 4329 (2015).

12. K. Jagadish, Y. Shiralgi, B.N. Chandrashekar, B.L. Dhananjaya, S. Srikantaswamy, in *Impact of Nanoscience in the Food Industry*, ed. Alexandru Mihai Grumezescu, Alina Maria Holban (Elsevier, New York, 2018), p. 197.
13. J.M. Blair, M.A. Webber, A.J. Baylay, D.O. Ogbolu, and L.J. Piddock, *Nat. Rev. Microbiol.* 13, 42 (2015).
14. L. Rizzo, C. Manaia, C. Merlin, T. Schwartz, C. Dagot, M. Ploy, I. Michael, and D. Fatta-Kassinos, *Sci. Total Environ.* 447, 345 (2013).
15. H. Heuer, H. Schmitt, and K. Smalla, *Curr. Opin. Microbiol.* 14, 236 (2011).
16. M.J. Hajipour, K.M. Fromm, A.A. Ashkarran, D.J. de Aberasturi, I.R. de Larramendi, T. Rojo, V. Serpooshan, W.J. Parak, and M. Mahmoudi, *Trends Biotechnol.* 30, 499 (2012).
17. X. Li, S.M. Robinson, A. Gupta, K. Saha, Z. Jiang, D.F. Moyano, A. Sahar, M.A. Riley, and V.M. Rotello, *ACS Nano* 8, 10682 (2014).
18. W. Gao, Y. Chen, Y. Zhang, Q. Zhang, and L. Zhang, *Adv. Drug Deliv. Rev.* 127, 46 (2017).
19. Y. Feng, W. Chen, Y. Jia, Y. Tian, Y. Zhao, F. Long, Y. Rui, and X. Jiang, *Nanoscale* 8, 13223 (2016).
20. B. Das, S.K. Dash, D. Mandal, J. Adhikary, S. Chattopadhyay, S. Tripathy, A. Dey, S. Manna, S.K. Dey, D. Das, and S. Roy, *BLDE Univ. J. Health Sci.* 1, 89 (2016).
21. T. Kalaiyarasan, V.K. Bharti, and O. Chaurasia, *RSC Adv.* 7, 51130 (2017).
22. P. Logeswari, S. Silambarasan, and J. Abraham, *J. Saudi Chem. Soc.* 19, 311 (2015).
23. M. Lv, S. Su, Y. He, Q. Huang, W. Hu, D. Li, C. Fan, and S.-T. Lee, *Adv. Mater.* 22, 5463 (2010).
24. T.-S. Kim, J.-R. Cha, and M.-S. Gong, *Text. Res. J.* 88, 766 (2018).
25. R.S. Santos, C. Figueiredo, N.F. Azevedo, K. Braeckmans, and S.C. De Smedt, *Adv. Drug Deliv. Rev.* 136, 28 (2018).
26. H.-L. Su, C.-C. Chou, D.-J. Hung, S.-H. Lin, I.-C. Pao, J.-H. Lin, F.-L. Huang, R.-X. Dong, and J.-J. Lin, *Biomaterials* 30, 5979 (2009).
27. S.A. Ansari, and Q. Husain, *Biotechnol. Adv.* 30, 512 (2012).
28. S. Mishra, N.G. Shimpi, and T. Sen, *J. Polym. Res.* 20, 49 (2013).
29. K. Ankireddy, S. Vunnam, J. Kellara, and W. Cross, *J. Mater. Chem. C* 1, 572 (2013).
30. S. Taheri, A. Cavallaro, S.N. Christo, P. Majewski, M. Barton, J.D. Hayball, K. Vasilev, and A.C.S. Biomater, *Sci. Eng.* 12, 1278 (2015).
31. J.A. LaNasa, V.M. Torres, and R.J. Hickey, *J. Appl. Phys.* 127, 134701 (2020).
32. K.H. Mahmoud, *Spectrochim. Acta Part A Mol. Biomol. Spectrosc.* 138, 434 (2015).
33. M. Moritz, and M. Geszke-Moritz, *Chem. Eng. J.* 228, 596 (2013).
34. R.J. Pinto, S.C. Fernandes, C.S. Freire, P. Sadocco, J. Causio, C.P. Neto, and T. Trindade, *Carbohyd. Res.* 348, 77 (2012).
35. Y. Delgado-Beleño, C. Martínez-Núñez, M. Cortez-Valadez, N. FloresLópez, and M. Flores-Acosta, *Mater. Res. Bull.* 99, 385 (2018).
36. A. Gonzalez, and C. Noguez, *J. Comput. Theor. Nanosci.* 4, 231 (2007).
37. N. Bogdanchikova, I. Tuzovskaya, A. Pestryakov, and A. Susarrey-Arce, *J. Nanosci. Nanotechnol.* 11, 5476 (2011).
38. J.-G. Bocarando-Chacon, M. Cortez-Valadez, D. Vargas-Vazquez, F. Rodríguez Melgarejo, M. Flores-Acosta, P.G. Mani-Gonzalez, E. LeonSarabia, A. Navarro-Badilla, and R. Ramírez-Bon, *Phys. E Low-Dimens. Syst. Nanostruct.* 59, 15 (2014).
39. P. Prieto, V. Nistor, K. Nouneh, M. Oyama, M. Abd-Lefdil, and R. Díaz, *Appl. Surf. Sci.* 258, 8807 (2012).
40. I. Lopez-Salido, D.C. Lim, and Y.D. Kim, *Surf. Sci.* 588, 6 (2005).
41. A. Saxena, R. Tripathi, F. Zafar, and P. Singh, *Mater. Lett.* 67, 91 (2012).
42. B. Le Ouay, and F. Stellacci, *Nano Today* 10, 339 (2015).
43. A. Nagy, A. Harrison, S. Sabbani, R.S. Munson Jr., P.K. Dutta, and W.J. Waldman, *Int. J. Nanomed.* 6, 1833 (2011).
44. M.M. Mohamed, S.A. Fouad, H.A. Elshoky, G.M. Mohammed, and T.A. Salaheldin, *Int. J. Vet. Sci. Med.* 5, 23 (2017).

Authors and Affiliations

Y. Delgado-Beleño[1,2] · C. E. Martínez-Núñez[1,2] · N. S. Flores-López[3] · A. Meza-Villezcas[4] · L. P. Ramírez-Rodríguez[5] · R. Britto Hurtado[1] · M. Flores-Acosta[1] · M. Cortez-Valadez[6]

Y. Delgado-Beleño
yoleivys.delgado@outlook.com

C. E. Martínez-Núñez
carlosmartinez0631@outlook.com

N. S. Flores-López
ns.flores@fata.unam.mx

A. Meza-Villezcas
amezaV@cicese.mx

M. Flores-Acosta
mario.floresacosta@unison.mx

M. Cortez-Valadez
jose.cortez@unison.mx

[1] Departamento de Investigación en Física, Universidad de Sonora, Apdo. Postal 5-88, 83190 Hermosillo, SON, Mexico

[2] Grupo de Espectroscopia Óptica y Láser, Universidad Popular del Cesar, Apdo. Postal 200001, Valledupar, Cesar, Colombia

[3] Centro de Física Aplicada y Tecnología Avanzada (CFATA), Universidad Nacional Autónoma de México (UNAM), Blvd. Juriquilla 3000, Querétaro, Mexico

[4] Centro de Investigación Científica y de Educación Superior de Ensenada, Ensenada, Baja California, Mexico

[5] Departamento de Física, Universidad de Sonora, Blvd. Luis Encinas y Rosales S/N, Col. Centro., 83000 Hermosillo, Sonora, Mexico

[6] CONACYT-Departamento de Investigación en Física, Universidad de Sonora, Apdo. Postal 5-88, 83190 Hermosillo, SON, Mexico